Near Infrared Plasmonic Optical Trapping Based on Hybrid Metal Nanorod

Zhiyun Li[1], **Zhinan Wang**[1], **Pengfei Cao**[1, 2], **Yongji Guan**[1], **Lin Cheng**[1], **and Linshan Chen**[3]

[1]School of Information Science and Engineering, Lanzhou University, Lanzhou 730000, China
[2]Kirchhoff-Institute for Physics, Im Neuenheimer Feld 227, Heidelberg 69120, Germany
[3]LDPE Plant, Lanzhou Petrochina Company, Lanzhou 730030, China

Abstract— The hybrid metal subwavelength structure which takes advantage of two different noble metals in their structures have become increasingly important as they can combine plasmonic dipole peaks associated with palladium (Pd) as well as silver (Ag), and thereby create additional plasmonic peaks. The additional peaks can provide a higher degree of control over the tunability of nanorods resonance and can potentially be beneficial in strong optical trapping application. With that in mind, in this paper, we introduce a near infrared plasmonic resonance (NIR) optical trapping based on hybrid nanorod pair array structure consisting of Pd and Ag metallic nanorods. The near infrared surface plasmons can be excited by using the hybrid metals subwavelength structure under the NIR wavelength. When the surface Plasmon (SP) wave impinges on the surfaces of hybrid metal injection molding (MIM), the two surface plasmon polaritons (SPPs) can be excited and propagate along the Pd and Ag surfaces. The constructive interference of these surface plasmons launched by the subwavelength hybrid structure can form an intense light field. The relationship between the incident wavelength, the distance of the Pd and Ag nanorod, and the forming intense light field are discussed in detail in order to design the optimal performance optical trapping structure for practical application. Based on Maxwell stress tensor method and numerical simulations, the maximum of optical force was calculated to be about 6.6 nN with input power 50 mW. The proposed nanostructure has great potential to trap nanoparticles and may be easily integrated into a small chip because of its simple structure for lab-on-a-chip applications.

1. INTRODUCTION

Since optical tweezers were first introduced by Ashkin et al. in 1986 [1], they have become an indispensable tool for noninvasively, disconnectedly and accurately capturing and manipulating a variety of particles and biological specimens [2, 3]. Unfortunately, traditional optical traps face trapping size limitations based on the diffraction limits; in particular, considering an object of radius equaling to R, the trapping efficiency drops rapidly (following an R^3 law). Therefore, nanoscale objects escape easily due to their physical sizes is smaller than the potential well of trap. One can overcome this reduction in force by increasing the optical power to strengthen the trap. However, samples typically undergo quick photo damage at high optical powers.

To overcome diffraction-limit, near field optical manipulation techniques have been developed; these techniques exploit the strong forces that can be generated in the near-field of SP structures. By using either propagating SPPs or localized surface plasmon resonance at a metal-dielectric interface [4], these SP tweezers can achieve trapping of submicrometer particles at a low optical power density. Several studies [5] recently have demonstrated that the plasmonic optical trapping can require the illumination power to remain below 10 mW. However, the force range available to plasmonic tweezers limits their applicabilities, with trapping forces usually spanning from subpiconewtons to approximately 1 pN. This range is compatible with the forces that individual molecular machines generate [6], but the mechanical characterization of macromolecules, their assemblies or more complex cellular processes can require much larger forces. For example, protein unfolding, amyloid fibril disruption, cell adhesion and contraction forces may be at the level of a nanonewton or more, which is beyond the capabilities of a SP tweezers [7]. Therefore, the problem is how to create the efficient SP tweezers that provide a strong optical force with low illumination power.

In this work, we present a more direct approach to create a nanonewton optical force trap by low power illuminating a hybrid palladium-silver nanorod pair array (Pd-AgNPA) deposited on double-deck substrate of calcium fluoride and silicon and study the trapping behavior of the nanospheres under such optical trap. Indeed, the optical properties of metal subwavelength structures, especially those of the noble metals Au, Ag, and Cu, exhibit unique Surface Plasmon Resonance (SPR) signatures. The hybrid metal subwavelength structure has become increasingly important as they

can combine plasmonic dipole peaks associated with Pd as well as Ag, and thereby create additional plasmonic peaks. The additional peaks can provide a higher degree of control over the tunability of nanorods resonance and can potentially be beneficial in strong optical trapping application. The near infrared surface plasmons (NISP) can be excited by using the hybrid metals subwavelength structure under the near infrared plasmonic resonance (NIR) wavelength. When the NISP wave impinges on the surfaces of hybrid metal subwavelength structure, the two SPPs can be excited and propagate along the Pd and Ag surfaces. The constructive interference of these surface plasmons launched by the hybrid metal subwavelength structure can form an intense light field. The commercial software "Comsol Multiphysics" was adopted here for the computational calculation [8]. The full wave simulations illustrate that when NIR occurs, the maximum of optical force is calculated to be about 6.6 nN by using Maxwell stress tensor with input power 50 mW. In contrast to other plasmonic tweezers, our Pd-AgNPA permits particle trapping, manipulating or complex cellular processes. The proposed nanostructure has great potential to trap nanoparticles and may be easily integrated into a small chip because of its simple structure for lab-on-a-chip applications.

2. METHODOLOGY

Figure 1(a) shows the structure of the proposed Pd-AgNPA. The structural parameters are diameter D, height H, and the center distance between the twonano-cylinders s, respectively. The Pd-AgNPAs are deposited on the double-deck substrates of calcium fluoride ($n = 1.43$) and silicon ($n = 3.48$) with the thin SiO_2 layer ($n = 1.5$, thickness is 120 nm). The environment is oil ($n = 1.55$) containing free nanoparticles ($n = 1.59$, the radius of the particle r is 80 nm). The relative permittivity of Pd and Ag is based on reported Lorentz-Drude model [9]. The light source is a plane wave illuminating from the top along the normal direction with electric field (amplitude 1 V/m) polarized along the y-axis. Fig. 1(b) shows typical resonance peak spectra at the center of the two nano-cylinders as appropriate structural parameters are chosen, namely, $H = 205$ nm, $D = 145$ nm, $s = 74.5$ nm in order to produce a narrow dominating NIR resonance peak at $\lambda = 810$ nm resulting from the excitation of SPPs and plasmonic interference within the hybrid nano-cylinders array. The reason is that the hybrid metal subwavelength structure can combine plasmonic dipole peaks associated with palladium (Pd) as well as silver (Ag), and thereby create additional NIR plasmonic peaks. When the NIR SP wave impinges on the surfaces of hybrid Pd-AgNPA, the two SPPs can be excited and propagate along the Pd and Ag surfaces. The constructive interference of these surface plasmons launched by the subwavelength hybrid metal structure can form an intense light field. Such highlight field is crucial in optical trapping applications to relax the power budget constraints.

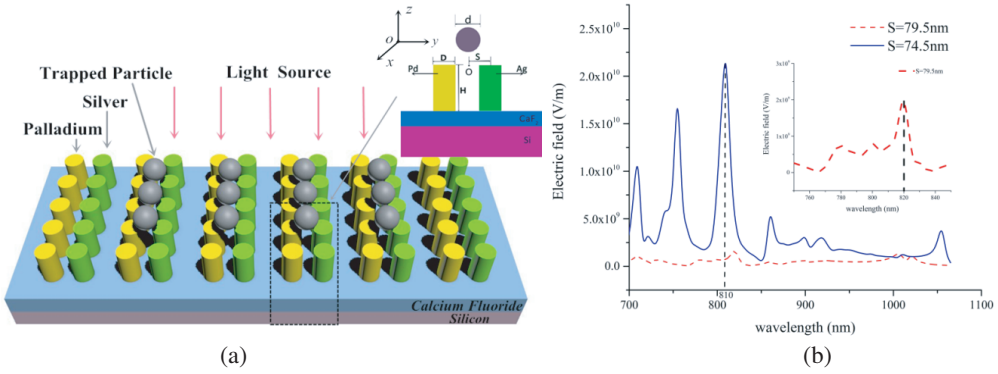

(a) (b)

Figure 1: (a) Schematic of the Pb-AgNPAs deposited on the double-deck substrate, showing the geometrical parameters defining the structure, as well as the y-z cross section is depicted at the top right corner. (b) The Transmission spectra of component Ez of the nanorod pair array along with the incident wavelength.

To determine the total induced optical force on a particle, we use the Maxwell stress tensor formalism [10]. The Maxwell's surface stress tensor (MST, $\langle T \rangle$) formalism [11] is used to determine the total optical force on a particle. The time averaged $\langle T \rangle$ is defined by:

$$\langle T \rangle = \frac{1}{2}\mathrm{Re}\left[\varepsilon EE^* + \mu HH^* - \frac{1}{2}\left(\varepsilon |E|^2 + \mu |H|^2\right) I\right] \tag{1}$$

where I denotes the identity matrix; EE^* and HH^* are the electric and magnetic field, respectively; ε and μ are the permittivity and the permeability of the surrounding medium, respectively. The components of the total time-averaged electromagnetic force F acting on the particle interacting with an optical field can be calculated using a surface integral [12]:

$$F = \oint \langle T \rangle \cdot dS \tag{2}$$

Thus, the total optical force on the particle can be obtained by calculating the electromagnetic fields over the bounding surface around the particle. The trapping potential resulting from the optical forces determines the stability of the optical trap. This potential can be directly obtained from:

$$U(x) = \left| \int_{\infty}^{x} F(r)dr \right| \tag{3}$$

In principle, a 1 kT (k is Boltzmann's constant, and T is the temperature) trapping potential well is sufficient to overcome the Brownian motion caused by the thermal energy of the particle and localize it in the optical trap. However, it has been proposed that stable optical trapping should require a potential well depth of approximately 10 kT [13]. In this work, we consider 10 kT as the threshold for stable optical trapping.

3. SIMULATION AND DISCUSSION

Figure 2 shows the electric field distribution with optical trapping in the yz plane. To evaluate the performance of the Pb-AgNPAs, we consider three figures of merit (FOM). The first two are optical trapping force and trapping potential. The last one is attenuation of the maximum electric field value, which can reflect the change of the Pb-AgNPAs capture capability with distance. Firstly, the distance between the particle and the Pb-AgNPAs was fixed to nm, while the position of the particle was swept over the xy plane to calculate the optical force field on the particle. The fields of the two transverse optical force components (F_x and F_y) exerted on the particle are shown in Fig. 3(a). The figures indicate that the two transverse force components work to localize the particle at the center of the Pb-AgNPAs. Actually the optical force can be readily tuned by varying the center distance s. Increasing or reducing the s will change the optical force. The choice of 74.5 nm is optimal distance of obtaining maximum optical force. When the particle is exactly at the center of the Pb-AgNPAs, the total transverse force acting on the particle is close to zero. As the particle tries to move away from the high-intensity region, due to Brownian motion or any other external force, the transverse forces restore it back to the equilibrium position in the center of the Pd-AgNPA. Note that the peak value of the force at the y-direction center ($F_{y\,\max} = 0.11\,\text{nN}/50\,\text{mW}$) does not equal zero. The reason is that the intensity of Pd nano-cylinder is bigger than that of Ag nano-cylinder at the resonant condition, which leads to the total optical force not equaling to zero.

The transverse forces result in a trapping potential well, as illustrated in Fig. 4. Figs. 4(a) and (b) show cross sections of the trapping potential well along $y = 0$ and $x = 0$ nm respectively. The depths of the well are $7.2 * 10^4$ kT per 5 mW and $6.3{*}10^4$ kT per 50 mW of transmitted power at room temperature along x direction and y direction, respectively. Since a 10 kT deep well is sufficient to stably trap a particle, trapping this 8 nm dielectric particle located the surface of

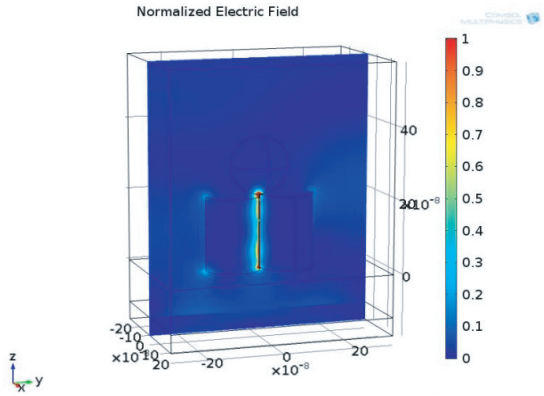

Figure 2: Electric field distribution with optical trapping in the yz plane.

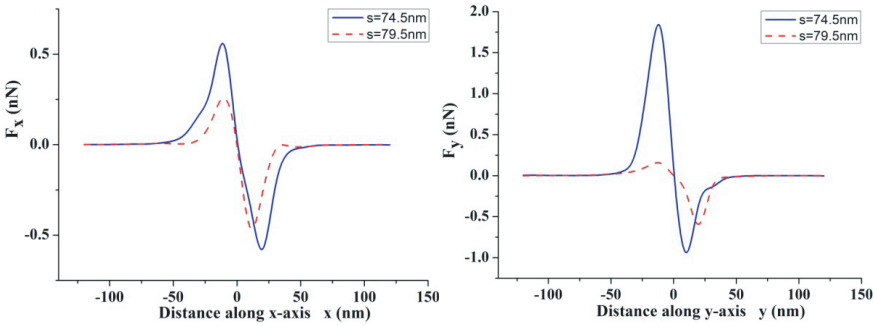

Figure 3: Cross sections of the transverse optical force components (a) F_x and (b) F_y.

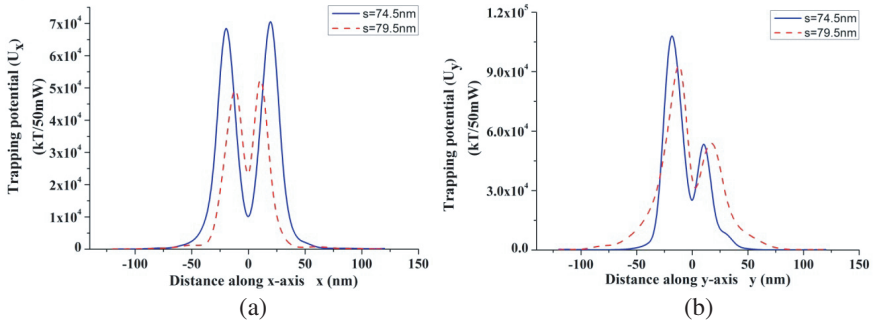

Figure 4: Cross sections of the transverse optical trapping potential (a) U_x and (b) U_y.

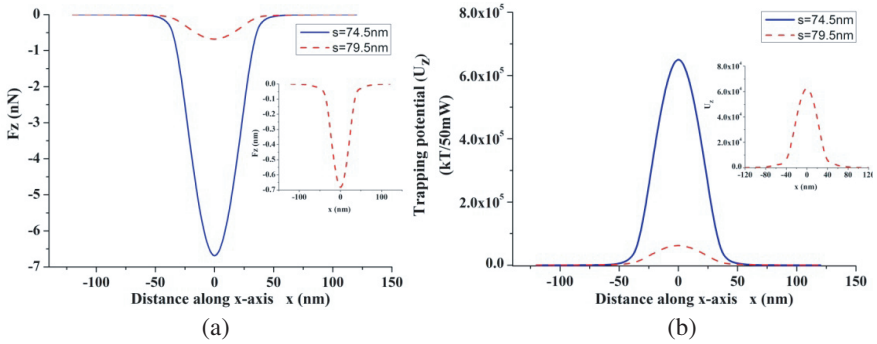

Figure 5: Cross sections of (a) the optical force F_z and (b) the optical trapping potential U_z along x direction.

the Pb-AgNPAs in the xy plane requires 50 mW of transmitted optical power. Along with the transverse localization forces, the particle also experiences a normal force component (F_z) which pulls the particle toward the Pb-AgNPAs. Comparing the x and y direction potential well with the pulling force profile reveals that the pulling force reaches its peak (6.6 nN/50 mW) right at the particle transverse equilibrium position, as shown in Fig. 5(a). The trapping potential profile of U_z is shown in Fig. 5(b) along with the transverse trapping direction (x direction). The changes of F_z and U_z along y direction are consistent with the F_z and U_z along x direction. This resultant force drags the particle toward the Pd-AgNPAs, where the x and y direction trapping forces are even stronger resulting in a stiffer trapping potential. We also explore the distance between the particle and the trapping structure on the optical forces.

Figures 6(a) and (b) illustrate the depth of the F_z and U_z along the z-axis as a function of the distance (z) measured the particle far away to the cylinders center. The figure indicates an exponential increase in optical forces as the targeted particle approaches the Pb-AgNPAs. However, with this design, the range of optical trapping along z-axis will be very small. The reason is that the widespread of the SPP with this design is small. Fig. 6(b) illustrates the change of the U_z decay with distance along z-axis. The reason is that an exponential attenuation in electric field as the SPP wave is far away from the Pd-AgNPAs. The intensity between the two cylinders is strongest, and the intensity at the cylindrical edge is the second. This result arises from the weaker

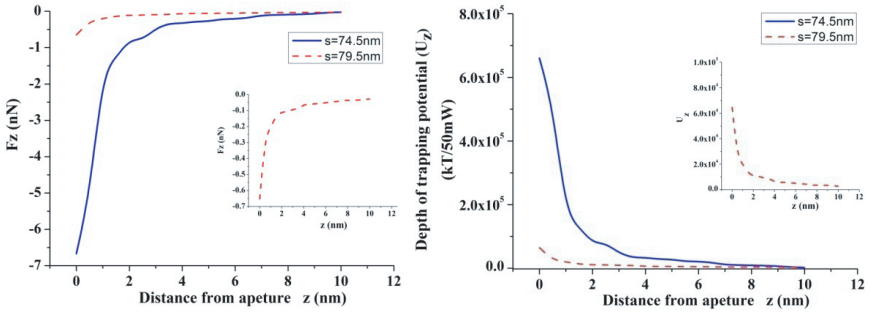

Figure 6: Cross sections of (a) the optical force F_z and (b) the optical trapping potential U_z along z direction.

confinement of the field in the z direction, as corresponded with the aforementioned figures. One of the easy methods to increase trapping range is to increase the required trapping power budget.

4. CONCLUSION

In conclusion, we have numerically demonstrated a hybrid palladium-silver nanorod pair array device operating at $\lambda = 810$ nm for 3D NIR optical trapping of nanoparticles. The device exhibits stable trapping performance and has a very large trapping force of approximately 6.6 nN, thus providing effective manipulation of nano-objects at very low incidence power into the high-field region and offering application potential in the field of microfluidics and lab-on-a-chip for biodetection.

ACKNOWLEDGMENT

The authors gratefully acknowledge financial support from the National Natural Science Foundation of China (No. 61205204), the "Spring Sunshine" Plan (No. Z2011029), the Open Research Fund of the State Key Laboratory of Transient Optics and Photonics, Chinese Academy of Sciences (No. SKLST201107) and the Fundamental Research Funds for the Central Universities.

REFERENCES

1. Ashkin, A., J. M. Dziedzic, J. E. Bjorkholm, et al., "Observation of a single-beam gradient force optical trap for dielectric particles," *Optics Letters*, Vol. 11, No. 5, 288–290, 1986.
2. Haruff, H. M., J. Munakata-Marr, and D. W. M. Marr, "Directed bacterial surface attachment via optical trapping," *Colloids. Surf. B*, Vol. 27, No. 2-3, 189–195, 2003.
3. Ashkin, A. and J. M. Dziedzic, "Optical trapping and manipulation of viruses and bacteria," *Science*, Vol. 235, No. 4795, 1517–1520, 1987.
4. Barnes, W. L., A. Dereux, and T. W. Ebbesen, "Surface plasmon subwavelength optics," *Nature*, Vol. 424, No. 6950, 824–830, 2003.
5. Dionne, J. A. and A. A. E. Saleh, "Method and structure for plasmonic optical trapping of nano-scale particles," U.S. Patent 20,160,049,215[P]. 2016-2-18.
6. Fazal, F. M. and S. M. Block, "Optical tweezers study life under tension," *Nature Photonics*, Vol. 5, No. 6, 318–321, 2011.
7. Veerapandian, M. and K. Yun, "Study of atomic force microscopy in pharmaceutical and biopharmaceutical interactions-A mini review," *Current Pharmaceutical Analysis*, Vol. 5, No. 3, 256–268, 2009.
8. Wang, J., B. Archambault, Y. Xu, et al., "Numerical simulation and experimental study on Resonant Acoustic Chambers — For novel, high-efficiency nuclear particle detectors," *Nuclear Engineering and Design*, Vol. 240, No. 11, 3716–3726, 2010.
9. Bohren, C. F. and D. R. Huffman, *Absorption and Scattering of Light by Small Particles*, John Wiley & Sons, 2008.
10. Stratton, J. A., *Electromagnetic Theory*, John Wiley & Sons, 2007.
11. Novotny, L., "Forces in optical near-fields," *Near-field Optics and Surface Plasmon Polaritons*, 123–141, Springer Berlin Heidelberg, 2001.
12. Barton, J. P. and D. R. Alexander, "Fifth-order corrected electromagnetic field components for a fundamental Gaussian beam, *Journal of Applied Physics*, Vol. 66, No. 7, 2800–2802, 1989.
13. Saleh, A. A. E. and J. A. Dionne, "Toward efficient optical trapping of sub-10-nm particles with coaxial plasmonic apertures," *Nano Letters*, Vol. 12, No. 11, 5581–5586, 2012.